JOURNAL OF MOLECULAR SPECTROSCOPY **181,** 108–118 (1996)
ARTICLE NO. MS967145

An *ab initio* Calculation of the Dipole Moment Surfaces and the Vibrational Transition Moments of the H_2Te Molecule

Igor N. Kozin,* Per Jensen,* Yan Li,* Robert J. Buenker,* Gerhard Hirsch,* and Stefan Klee†

*FB 9-Theoretische Chemie, Bergische Universität, Gesamthochschule Wuppertal, D-42097 Wuppertal, Germany; and
†Physikalisch-Chemisches Institut, Justus-Liebig-Universität, Heinrich-Buff-Ring 58, D-35392 Giessen, Germany

Received April 23, 1996; in revised form August 2, 1996

The present work reports an *ab initio* MRD-CI calculation of the dipole moment surfaces for the electronic ground state of the H_2Te molecule. Using the *ab initio* results, we calculate the vibrational transition moments, and we simulate the far-infrared spectrum of H_2Te by means of the MORBID program system. We obtain the equilibrium value of the dipole moment from the *ab initio* calculation as 0.377 Debye based on our initial theoretical treatment which was employed over a wide range of molecular geometries. However, the use of an improved AO basis at the equilibrium geometry of H_2Te lowers this result to 0.298 Debye. The comparison of our simulated far-infrared spectrum with the experimental spectrum suggests that this value is too large, and that the correct value is certainly larger than 0.19 Debye and very probably smaller than 0.26 Debye. From the *ab initio* data, we predict many vibrational transition moments for H_2Te, D_2Te, and HDTe. We hope that these results will be of assistance in the interpretation of the rotation–vibration spectrum of these molecules.

I. INTRODUCTION

Fairly recently, it has been realized that the water-type molecules H_2S, H_2Se, and H_2Te have an initially unexpected energy level structure in that at high J and K_a values, the rotational energies form groups of four nearly degenerate levels. This so-called energy cluster formation is the subject of the review in (*1*), and the reader is referred to that paper, and to the references cited in it, for a thorough discussion of the energy clusters in H_2S, H_2Se, and H_2Te, and of our present knowledge about the highly excited rotational levels in H_2O. The cluster formation has been experimentally verified for the vibrational ground state (see Refs. (*2, 3*) and the references cited in them) and the ν_1/ν_3 vibrational states (*4*) of H_2Se and, very recently, for the vibrational ground state[1] and for excited stretching states[2] of H_2S. The results obtained for H_2S and H_2Se have stimulated experimental (*5–7*) and theoretical (*1, 8*) studies of the related molecule H_2Te. At present, extensive analyses of newly recorded Fourier transform infrared spectra of H_2Te are being carried out. They involve the ν_2 band (*6*) and the stretching fundamental transitions together with several overtone and combination bands (*7*). For the analysis of these infrared spectra, precise rotation–vibration parameters for the vibrational ground state are required. Such parameters have been obtained from the far infrared spectrum of H_2Te, recorded with a Fourier transform spectrometer (*5*). In order to improve the accuracy of the ground state rotation–vibration constants, it is desirable to supplement the far-infrared Fourier transform data of Ref. (*5*) by information from submillimeter-wave spectra. Toward this end, the submillimeter-wave spectrum of H_2Te is presently being measured (*9*). In these experiments, each transition must be located in a time-consuming search, which obviously can be much facilitated if accurate predictions of the transition frequencies are available. For H_2Te, we can obtain such predictions from the molecular parameters determined in Ref. (*5*). However, it is also essential that the transition intensities can be reliably estimated. With such estimations, it can be decided whether the detection of a particular transition is feasible so that it is reasonable to search for it.

In the present work, we report an *ab initio* calculation of the dipole moment surfaces for the electronic ground state, and of the corresponding rotation–vibration transition moments and intensities of H_2Te. The principal aim of this work is to provide theoretical intensity values facilitating the search for rotational transitions of H_2Te. However, we calculate also the vibrational transition moments for a selection of vibrational transitions of H_2Te and hope that these results will be of assistance in the interpretation of the rotation–vibration spectrum.

II. THE *ab initio* CALCULATION OF THE DIPOLE MOMENT VALUES

In our previous *ab initio* calculation of the potential energy surface for the electronic ground state of H_2Te (*8*), we used

[1] O. L. Polyansky, S. Klee, G. Ch. Mellau, J. Demaison, and P. Jensen, Poster B17, Fourteenth Colloquium on High Resolution Molecular Spectroscopy, Dijon, France, September 1995.

[2] L. R. Brown, J. Crisp, D. Crisp, A. Bykov, O. Naumenko, M. Smirnov, L. Sinitsa, and A. Perrin, Poster F14, Fourteenth Colloquium on High Resolution Molecular Spectroscopy, Dijon, France, September 1995.

0022-2852/97 $25.00

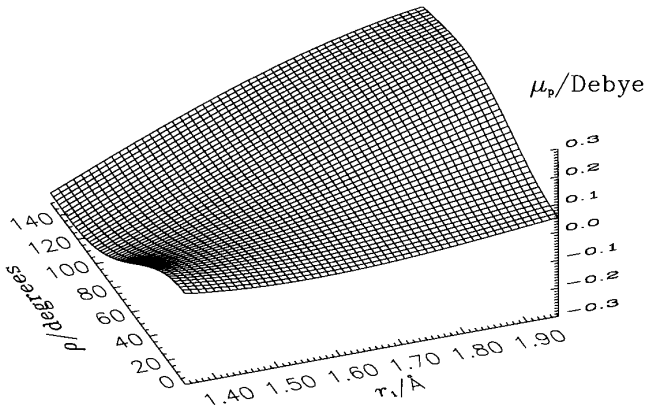

FIG. 1. The dipole moment component μ_p (see Eq. [1]) shown as a function of the bond angle supplement ρ and the bond length r_1. The bond length r_3 is held fixed at its equilibrium value.

the CCSD(T) *ab initio* method (*10*) as implemented in the TITAN *ab initio* program.[3] However, the TITAN program package available to us does not provide values of the electronically averaged dipole moment components, so the present calculation was carried out with the MRD-CI program package (*11–16*), employing a relativistic effective core potential (RECP). Only the $4d$, $5s$, and $5p$ shells of Te are included in the active space in both the SCF and CI computations. The Te RECP is taken from Hurley *et al.* (*17*). A [$4s$, $4p$, $3d$] contracted Cartesian Gaussian basis was taken from those recommended for use with the RECP chosen for Te (*17*). An additional calculation at the H_2Te equilibrium geometry has also been carried out with an improved AO basis containing two more Te d functions. A [$3s$] contracted basis augmented with two sets of p orbitals was chosen for the H atom (*18*). The dipole moment components of the electronic ground state of the H_2Te molecule were calculated for 153 molecular geometries with internuclear distances from 2.60 to 3.80 a_0 and H–Te–H bond angles from 70° to 110°.

III. FITTING THE DIPOLE MOMENT FUNCTIONS

The calculated dipole moment components are measured relative to the p and q axes defined in Fig. 1 of Ref. (*19*). The pq axis system has origin at the nuclear center of mass, and the p and q axes are in the plane defined by the three nuclei. The q axis bisects the bond angle α and points so that the q coordinates of the ''terminal'' nuclei 1 and 3 are positive. The p axis is perpendicular to the q axis and points so that the p coordinate of nucleus 3 is positive. The dipole moment component along the p axis, μ_p, was expanded as

$$\mu_p(\Delta r_1, \Delta r_3, \bar{\rho}) = \mu_0^{(p)}(\bar{\rho}) + \sum_j \mu_j^{(p)}(\bar{\rho})\Delta r_j + \sum_{j\leqslant k} \mu_{jk}^{(p)}(\bar{\rho})\Delta r_j \Delta r_k + \sum_{j\leqslant k\leqslant m} \mu_{jkm}^{(p)}(\bar{\rho})\Delta r_j \Delta r_k \Delta r_m + \sum_{j\leqslant k\leqslant m\leqslant n} \mu_{jkmn}^{(p)}(\bar{\rho})\Delta r_j \Delta r_k \Delta r_m \Delta r_n, \quad [1]$$

where all of the indices j, k, m, and n assume the values 1 or 3. In Eq. [1], $\Delta r_j = r_j - r_j^e$, $j = 1$ or 3, is defined as a displacement from the equilibrium value r_j^e of the distance r_j between the ''outer'' nucleus $j = 1$ or 3 and the ''center'' nucleus 2. The quantity $\bar{\rho} = \pi - \alpha$ is the instantaneous value of the bond angle supplement (see Fig. 1 of Ref. (*20*)). Further,

$$\mu_{jk\ldots}^{(p)}(\bar{\rho}) = \sum_{i=0}^{N} p_{jk\ldots}^{(i)} (\cos\rho_e - \cos\bar{\rho})^i, \quad [2]$$

where the $p_{jk\ldots}^{(i)}$ are molecular parameters and ρ_e is the equilibrium value of $\bar{\rho}$. The function $\mu_0^{(p)}(\bar{\rho})$ has $N = 8$, $\mu_j^{(p)}(\bar{\rho})$ has $N = 4$, $\mu_{jk}^{(p)}(\bar{\rho})$ has $N = 3$, $\mu_{jkm}^{(p)}(\bar{\rho})$ has $N = 2$, and $\mu_{jkmn}^{(p)}(\bar{\rho})$ has $N = 1$.

The dipole moment component along the q axis, μ_q, was represented by

$$\mu_q(\Delta r_1, \Delta r_3, \bar{\rho}) = \sin\bar{\rho}[\mu_0^{(q)}(\bar{\rho}) + \sum_j \mu_j^{(q)}(\bar{\rho})\Delta r_j + \sum_{j\leqslant k} \mu_{jk}^{(q)}(\bar{\rho})\Delta r_j \Delta r_k + \sum_{j\leqslant k\leqslant m} \mu_{jkm}^{(q)}(\bar{\rho})\Delta r_j \Delta r_k \Delta r_m + \sum_{j\leqslant k\leqslant m\leqslant n} \mu_{jkmn}^{(q)}(\bar{\rho})\Delta r_j \Delta r_k \Delta r_m \Delta r_n]. \quad [3]$$

Again, all of the indices j, k, m, and n assume the values 1 or 3. The equations for the $\mu_{jkm\ldots}^{(q)}(\bar{\rho})$ functions are obtained when p is replaced by q in Eq. [2].

In Eqs. [1]–[2], relations exist between the parameters $p_{jk\ldots}^{(i)}$ so that the function $\bar{\mu}^{(p)}(\Delta r_1, \Delta r_3, \bar{\rho})$ is antisymmetric under the interchange of Δr_1 and Δr_3. Similarly, relations exist between the parameters $q_{jk\ldots}^{(i)}$ so that the function $\bar{\mu}^{(q)}(\Delta r_1, \Delta r_3, \bar{\rho})$ is invariant under the interchange of Δr_1 and Δr_3.

We obtain values for the $p_{jk\ldots}^{(i)}$ and $q_{jk\ldots}^{(i)}$ parameters by fitting Eqs. [1] and [3] through the *ab initio* dipole moment values. For μ_q we used 9 parameters to fit the 153 nonvanishing dipole moment values. The standard deviation of the fitting was 0.0315 Debye. For μ_p we used 7 parameters to fit the 122 nonvanishing dipole moment values. The standard deviation of this fitting was 0.0384 Debye. The dipole mo-

[3] TITAN is a set of electronic structure programs written by T. J. Lee, A. P. Rendell, and J. E. Rice.

TABLE 1
Fitted Dipole Moment Parameters for H_2Te

The μ_q component		The μ_p component	
$q_0^{(0)}$/Debye	0.3772(23)	$p_1^{(0)}$/Debye Å^{-1}	0.7493(142)
$q_0^{(1)}$/Debye	−0.9858(87)	$p_1^{(1)}$/Debye Å^{-1}	0.3097(283)
$q_0^{(2)}$/Debye	0.9163(254)	$p_1^{(2)}$/Debye Å^{-1}	−0.3564(1038)
$q_1^{(0)}$/Debye Å^{-1}	−0.6589(61)	$p_{11}^{(0)}$/Debye Å^{-2}	−0.0836(346)
$q_1^{(1)}$/Debye Å^{-1}	0.5697(212)	$p_{11}^{(1)}$/Debye Å^{-2}	−0.5262(1407)
$q_1^{(2)}$/Debye Å^{-1}	−0.6118(953)	$p_{111}^{(0)}$/Debye Å^{-3}	−0.4712(1654)
$q_{11}^{(0)}$/Debye Å^{-2}	0.2788(231)	$p_{113}^{(0)}$/Debye Å^{-3}	−0.2381(1331)
$q_{11}^{(1)}$/Debye Å^{-2}	0.5739(1198)		
$q_{13}^{(0)}$/Debye Å^{-2}	−0.1924(328)		

ment parameters are given in Table 1. Figures 1 and 2 show cuts through the analytical functions representing the dipole moment components μ_p and μ_q, respectively.

IV. THE VIBRATIONAL TRANSITION MOMENTS

The dipole parameter values of Table 1 have been used as input for the MORBID intensity program (*19–23*), and we show in Tables 2–4 approximate vibrational transition moments calculated by this program for $H_2{}^{130}Te$, $D_2{}^{130}Te$, and $HD^{130}Te$, respectively. These transition moments are matrix elements between the vibrational basis functions

$$|N_{\text{vib}}\Gamma_{\text{Sym}};\, v_2,\, K\rangle = |N_{\text{vib}}\Gamma_{\text{Sym}}\rangle|v_2,\, K\rangle \qquad [4]$$

of the dipole moment components μ_y and μ_z in the molecule fixed *xyz* coordinate system defined by the Eckart and Sayvetz conditions given as Eqs. [10] and [11] of Ref. (*20*) (see also Fig. 1 of Ref. (*20*)). The *xyz* coordinate system has its origin at the center of mass and the nuclei lie in the *yz* plane; for linear configurations the *y* axis coincides with the *q* axis and the *z* axis (which, for a linear configuration, is the molecular axis) coincides with the *p* axis. In Eq. [4], the stretching basis functions $|N_{\text{Vib}}\Gamma_{\text{Sym}}\rangle$ are obtained as the eigenfunctions of the Hamiltonian $\hat{H}_{\text{Stretch}}$ (see Eq. [58] of Ref. (*20*)) by setting up the matrix of $\hat{H}_{\text{Stretch}}$ in a basis of symmetrized Morse oscillator functions as described in Section V of Ref. (*20*), and the bending basis functions $|v_2, K\rangle$ are the eigenfunctions of $\hat{H}_{\text{Bend}}$ (see Eq. [63] of Ref. (*20*)). These functions are obtained in a one-dimensional numerical integration procedure as described in Section V of Ref. (*20*). The signs of the transition moments in Tables 2–4 have no physical significance. They depend on the arbitrary relative phases of the basis functions.

In the calculation of the transition moments, the potential energy function of H_2Te was taken to be given by Eqs. [1]–[5] of Ref. (*1*) with the parameter values taken from Table I of Ref. (*1*). This potential energy surface was obtained in a least-squares fit (using the MORBID program) to experimental term values involving $J \leqslant 5$ from Refs. (*24–30*).

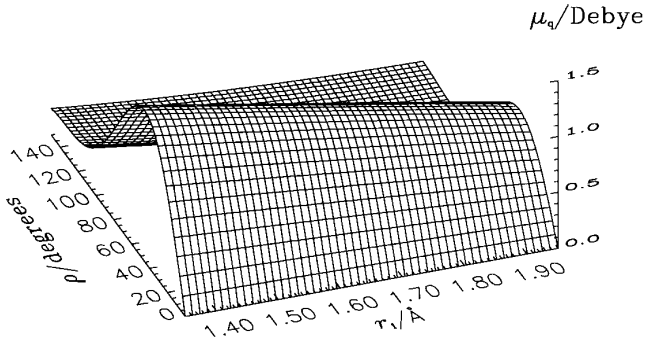

FIG. 2. The dipole moment component μ_q (see Eq. [3]) shown as a function of the bond angle supplement ρ and the bond length r_1. The bond length r_3 is held fixed at its equilibrium value.

V. A SIMULATION OF THE FAR INFRARED SPECTRUM OF H_2Te

In order to assess the accuracy of the *ab initio* dipole moment values calculated in the present work, we have used them to simulate the far-infrared spectrum of H_2Te recorded (*5*) with the Bruker IFS 120 HR Fourier transform spectrometer at the University of Giessen, Germany. This spectrum covers the wavenumber region 90–300 cm^{-1} and was recorded at an absolute temperature of $T = 233$ K. The absorption path length was $l = 302$ cm. The spectra were not apodized. The H_2Te molecules in the sample contained Te isotopes in natural abundance. The initial H_2Te pressure was measured as 5.01 mbar. However, the H_2Te molecule is unstable and decomposes substantially during the experiment. Consequently, it is necessary to determine the effective H_2Te concentration resulting from the sample decomposition taking place over the full duration of the experiment which was more than 11 hr. In spite of measuring at low temperature and under exclusion of ambient light, we observed, at the end of the experiment, a significant coating of the cell surface by elementary tellurium. The time evolution of the H_2Te partial pressure as well as its effective average value could be determined from the intensities of some representative absorption lines measured within the four subsequent blocks of individual scans that were added to yield the sum spectrum. The spectral line analysis was performed using Johns' INTBAT program (*31*). The intensities of the representative lines, which were

TABLE 2
Vibrational Transition Moments $\langle\psi''|\mu|\psi'\rangle$ (in Debye) for Selected Vibrational Transitions of $H_2{}^{130}Te$

v_1''	v_2''	v_3''	E''/cm^{-1}	v_1'	v_2'	v_3'	E'/cm^{-1}	$\langle\psi''\|\mu\|\psi'\rangle$
Matrix elements of μ_y[a]								
0	0	0	0.0	0	0	0	0.0	0.3687
				0	1	0	860.8	0.1105
				0	2	0	1731.7	0.0123
				1	0	0	2063.2	0.0827
				0	3	0	2609.7	−0.0023
				1	1	0	2911.4	0.0089
				0	4	0	3492.4	−0.0005
				1	2	0	3769.3	0.0002
				2	0	0	4063.1	−0.0121
				0	0	2	4132.3	0.0031
0	1	0	860.8	0	1	0	860.8	0.3890
				0	2	0	1731.7	0.1512
				1	0	0	2063.2	0.0087
				1	1	0	2911.4	0.0837
1	0	0	2063.2	1	0	0	2063.2	0.3473
0	0	1	2070.2	0	0	1	2070.2	0.3506
Matrix elements of μ_z[b]								
0	0	0	0.0	0	0	1	2070.2	−0.0919
				0	1	1	2916.0	0.0042
				0	2	1	3771.5	0.0059
				1	0	1	4063.2	−0.0111
0	1	0	860.8	0	0	1	2070.2	0.0042
				0	1	1	2916.0	−0.0906

[a]The matrix elements of μ_y have $K'' = 0$ and $K' = 1$.

[b]The matrix elements of μ_z have $K'' = K' = 0$.

TABLE 3
Vibrational Transition Moments $\langle\psi''|\mu|\psi'\rangle$ (in Debye) for Selected Vibrational Transitions of $D_2{}^{130}Te$

v_1''	v_2''	v_3''	E''/cm^{-1}	v_1'	v_2'	v_3'	E'/cm^{-1}	$\langle\psi''\|\mu\|\psi'\rangle$
Matrix elements of μ_y[a]								
0	0	0	0.0	0	0	0	0.0	0.3713
				0	1	0	611.8	0.0948
				0	2	0	1229.4	0.0091
				1	0	0	1480.7	0.0703
				0	3	0	1851.6	−0.0014
				1	1	0	2086.3	0.0063
				0	4	0	2477.5	−0.0003
				1	2	0	2697.6	0.0003
				2	0	0	2931.1	−0.0085
				0	0	2	2966.8	0.0026
0	1	0	611.8	0	1	0	611.8	0.3863
				0	2	0	1229.4	0.1309
				1	0	0	1480.7	0.0062
				1	1	0	2086.3	0.0709
1	0	0	1480.7	1	0	0	1480.7	0.3562
0	0	1	1486.2	0	0	1	1486.2	0.3585
Matrix elements of μ_z[b]								
0	0	0	0.0	0	0	1	1486.2	−0.0778
				0	1	1	2090.4	0.0031
				0	2	1	2700.3	0.0043
				1	0	1	2931.1	0.0076
0	1	0	611.8	0	0	1	1486.2	0.0031
				0	1	1	2090.4	−0.0770

[a]The matrix elements of μ_y have $K'' = 0$ and $K' = 1$.

[b]The matrix elements of μ_z have $K'' = K' = 0$.

TABLE 4
Vibrational Transition Moments $\langle\psi''|\mu|\psi'\rangle$ (in Debye) for Selected Vibrational Transitions of HD ^{130}Te

v_1''	v_2''	v_3''	E''/cm^{-1}	v_1'	v_2'	v_3'	E'/cm^{-1}	$\langle\psi''\|\mu_y\|\psi'\rangle^a$	$\langle\psi''\|\mu_z\|\psi'\rangle^b$
0	0	0	0.0	0	0	0	0.0	0.3576	0.0953
				0	1	0	746.6	0.1022	0.0193
				0	0	1	1483.0	0.0348	0.0654
				0	2	0	1501.3	0.0110	0.0002
				1	0	0	2066.8	−0.0727	0.0487
				0	1	1	2222.6	0.0066	−0.0017
				0	3	0	2262.0	−0.0018	−0.0008
				1	1	0	2799.6	−0.0041	−0.0028
				0	0	2	2930.9	0.0047	0.0068
				0	2	1	2970.1	0.0003	−0.0005
				0	4	0	3026.8	−0.0004	0.0000
				1	2	0	3539.8	−0.0003	−0.0005
				1	0	1	3548.4	−0.0010	−0.0005
				2	0	0	4064.0	0.0105	−0.0053
0	1	0	746.6	0	1	0	746.6	0.3758	0.0961
				0	0	1	1483.0	0.0065	−0.0017
				0	2	0	1501.3	0.1405	0.0257
				1	0	0	2066.8	−0.0040	−0.0028
				0	1	1	2222.6	0.0354	0.0646
				1	1	0	2799.6	−0.0732	0.0479
0	0	1	1483.0	0	0	1	1483.0	0.3485	0.0748
1	0	0	2066.8	1	0	0	2066.8	0.3324	0.1140

[a] The matrix elements of μ_y have $K'' = 0$ and $K' = 1$.

[b] The matrix elements of μ_z have $K'' = K' = 0$.

found to decrease steadily from block to block, could be fitted in a reasonable manner to a second-order polynomial in the time elapsed since the beginning of the experiment. By means of this polynomial, the intensities could be time averaged. From this procedure we obtain the H_2Te effective pressure as $P = (4.18 \pm 0.15)$ mbar.

The simulation of the experimental spectrum proceeds as follows: We use the theory and computer program described in Ref. (*19*) to calculate, for each rotation–vibration transition from an initial state $|\psi_i\rangle$ to a final state $|\psi_f\rangle$, the integrated absorption coefficient given by

$$I_{if} = \frac{8\pi^3 N_A g_{ns} \tilde{\nu}_{if} \exp(-E_i/kT) \times [1 - \exp(-hc\tilde{\nu}_{if}/kT)]}{3hcQ} S(f \leftarrow i), \quad [5]$$

where N_A is Avogadro's number, g_{ns} is the nuclear spin statistical weight, $\tilde{\nu}_{if}$ is the wavenumber of the transition (in cm^{-1}), E_i is the energy of the initial state, k is the Boltzmann constant, h is Planck's constant, c is the vacuum velocity of light, and the partition function Q is given by

$$Q = \sum_w g_w \exp(-E_w/kT). \quad [6]$$

In Eq. [6], E_w is the energy and g_w the total degeneracy of the state w and the summation extends over all such states of the molecule. The line strength $S(f \leftarrow i)$ of an electric dipole transition is defined as

$$S(f \leftarrow i) = \sum_{A=X,Y,Z} \sum_{M_i,M_f} |\langle\psi_f|\mu_A|\psi_i\rangle|^2, \quad [7]$$

where μ_A is the component of the electronically averaged molecular dipole moment operator along the A axis ($A = X, Y,$ or Z) of the space fixed coordinate system and M_i and M_f are the rotational M quantum numbers (quantizing the Z component of the total angular momentum) of the initial and final states, respectively.

The absorption lines will be broadened because of Doppler broadening and pressure broadening. At $T = 233$ K, the Doppler width (Half Width at Half Maximum, HWHM) of an $H_2{}^{130}Te$ transition with center wavenumber $\tilde{\nu}_{if}$ amounts to $4.8 \times 10^{-7} \times \tilde{\nu}_{if}$. That is, a line at 100 cm^{-1} will have a Doppler width of 4.8×10^{-5} cm^{-1}. This is negligibly small in comparison with the observed HWHM of the lines which is around 0.0007 cm^{-1}, and so we neglect Doppler broadening in the present work. For each line, we obtain the absorption coefficient $\epsilon(\tilde{\nu})$ of a pressure broadened line by multiplying the integrated absorption coefficient from Eq. [5] by a Lorentzian lineshape function

$$\epsilon(\tilde{\nu}) = I_{if} \frac{\Delta\tilde{\nu}_P}{\pi} \frac{1}{\Delta\tilde{\nu}_P^2 + (\tilde{\nu} - \tilde{\nu}_{if})^2}, \qquad [8]$$

where $\Delta\tilde{\nu}_P$ is the HWHM of the Lorentzian which is normalized so that

$$I_{if} = \int_{Line} \epsilon(\tilde{\nu}) d\tilde{\nu}. \qquad [9]$$

We can now calculate the absorbance of the line as

$$A(\tilde{\nu}) = c^* l \epsilon(\tilde{\nu}), \qquad [10]$$

where the concentration of absorbing molecules, c^*, is obtained from the ideal-gas equation (*32*)

$$c^* = \frac{P}{RT} \times a \qquad [11]$$

with R as the gas constant and $0 < a \leq 1$ as the abundance of the isotopomer in question. The absorbance is converted to transmittance

$$T(\tilde{\nu}) = \exp(-A(\tilde{\nu})) \qquad [12]$$

and, finally, the transmittance spectrum is convoluted with an instrumental lineshape function F_{ILS} given by (*33*)

$$F_{ILS}(\tilde{\nu}) = \frac{\sin(2\pi(\tilde{\nu}/\Delta\tilde{\nu}_{ILS}))}{\pi\tilde{\nu}}. \qquad [13]$$

The quantity $\Delta\tilde{\nu}_{ILS} = 1/\Delta_{MOPD}$, where Δ_{MOPD} is the maximum optical path difference attained during the recording of the Fourier transform spectrum. In the present experiment, we have $\Delta\tilde{\nu}_{ILS} = 0.00184$ cm^{-1}. The transmittance function obtained from the convolution can be compared directly with the experimental transmittance spectrum.

In the simulation of the far infrared spectrum, we have calculated the spectra of the isotopomers $H_2{}^{130}Te$ (0.3380), $H_2{}^{128}Te$ (0.3169), $H_2{}^{126}Te$ (0.1895), $H_2{}^{125}Te$ (0.0714), $H_2{}^{124}Te$ (0.0482), $H_2{}^{122}Te$ (0.0260), and $H_2{}^{123}Te$ (0.0091). For each isotopomer, we give in parentheses its natural abundance a (i.e., the natural abundance of the Te isotope in question) (*34*). The MORBID calculations were done with the potential energy function of Ref. (*1*), using a basis set in which the stretching problem was prediagonalized [see Ref. (*20*)] with Morse oscillator functions $|n_1 n_3\rangle$ having $n_1 + n_3 \leq N_{Stretch} = 7$. In constructing the final rotation–vibration matrices we used the $N_{Bend} = 8$ lowest bending basis functions, the $N_A = 6$ lowest stretching basis functions of A_1 symmetry, and the $N_B = 4$ lowest stretching basis functions of B_2 symmetry. For each isotopomer, the program attempts to generate all transitions (i.e., all transitions involving states that can be calculated with the given basis set and the given J_{max} value) with wavenumbers in the region from 100 to 300 cm^{-1} and with an integrated absorption coefficient (Eq. [5]) larger than 10^{-3} cm/mol. The partition function (Eq. [6]) is obtained by summation over all energies (converged or not converged) generated with the given basis set and J_{max} value. Owing to the very large number of possible transitions to be investigated, the MORBID calculation for one isotopomer required more than 50 hr of CPU time on an IBM RISC/6000 340 workstation with 32 MB RAM.

Initial calculations showed that the calculated transmittance values obtained from our simulations were systematically smaller than the corresponding experimental values. In order to investigate the deviations further we have selected a number of ''representative transitions'' from the spectrum. They are given in Table 5. These lines are sufficiently strong that the noise in the experimental spectrum is negligible over the line profile, but on the other hand they are not so strong as to be optically thick. Since the experimental linewidth changes slightly from line to line we compare in Table 5 calculated values for integrated absorbance, i.e.,

$$A = \int_{Line} A(\tilde{\nu}) d\tilde{\nu}, \qquad [14]$$

with the corresponding experimental values. Experimental linewidths and peak absorbances were derived using the SPECTRA program,[4] which allows an iterative fitting of an observed line profile to a Lorentzian function. It follows from Eqs. [8] and [9] that for a Lorentzian line we can calculate the experimental integrated absorbance as

[4] SPECTRA is a program written by M. Carleer, Laboratoire de Chimie Physique Moleculaire, Université Libre de Bruxelles, Belgium.

TABLE 5
Calculated and Experimental Values[a] of the Integrated Absorbance A for Selected Far-Infrared Transitions of H_2Te

$J'_{K'_aK'_c} \leftarrow J''_{K''_aK''_c}$	Isot.[b]	$\tilde{\nu}_{exp}$[c]	$\mathcal{A}_{calc}$	$\Delta\tilde{\nu}_{exp}$[d]	$(A_0)_{exp}$[e]	$\mathcal{A}_{exp}$	$\mathcal{A}_{calc}/\mathcal{A}_{exp}$
		cm^{-1}	cm^{-1}	cm^{-1}		cm^{-1}	
$11_{84} \leftarrow 10_{73}$	130	112.98	0.00465	0.000586	0.634	0.00117	3.98
	128	113.01	0.00436	0.000678	0.503	0.00107	4.07
$11_{83} \leftarrow 10_{92}$	130	114.76	0.00747	0.000635	0.891	0.00178	4.20
	128	114.74	0.00696	0.000682	0.805	0.00172	4.03
	126	114.73	0.00415	0.000679	0.493	0.00105	3.95
$11_{92} \leftarrow 10_{101}$	130	116.23	0.00280	0.000721	0.343	0.000776	3.60
	128	116.17	0.00258	0.000604	0.324	0.000614	4.20
$8_{53} \leftarrow 7_{44}$	130	119.29	0.00617	0.000753	0.623	0.00147	4.19
	128	119.30	0.00578	0.000736	0.618	0.00143	4.05
$12_{94} \leftarrow 11_{83}$	130	125.31	0.00749	0.000658	0.883	0.00183	4.10
	128	125.34	0.00700	0.000665	0.780	0.00163	4.30
	126	125.37	0.00419	0.000684	0.492	0.00106	3.96
$9_{73} \leftarrow 8_{44}$	130	131.54	0.00502	0.000664	0.560	0.00117	4.30
	128	131.56	0.00471	0.000750	0.513	0.00121	3.90
	126	131.57	0.00282	0.000743	0.286	0.000668	4.22

[a] From Ref. *(5)*.

[b] Mass number for the Te isotope of the H_2Te isotopomer in question.

[c] Experimental peak wavenumber from Ref. *(5)*.

[d] Half width at half maximum of the line, see the text.

[e] Experimental peak absorbance.

$$A = \Delta\tilde{\nu}\pi A_0, \qquad [15]$$

where $\Delta\tilde{\nu}$ is the HWHM of the Lorentzian profile and A_0 is the peak absorbance. For the lines in Table 5, we form the ratio of calculated integrated absorbance to observed integrated absorbance, $\mathcal{A}_{calc}/\mathcal{A}_{exp}$. The table shows that this ratio lies in the region from 3.6 to 4.3 with an average value of 4.07. We shall discuss the possible reasons for the discrepancies below. We have made a simulation of the H_2Te far-infrared spectrum in which we use the linewidth (Eq. [8]) $\Delta\tilde{\nu}_P = 0.000682\ cm^{-1}$, the average linewidth for the transitions in Table 5. Further, we empirically reduce our calculated absorbances by a factor of 4.07. Parts of the simulations are shown in Figs. 3 and 4. The experimental H_2Te spectrum which we simulate here has all-pervading strong absorptions of H_2O and H_2S, and the two wavenumber intervals shown in the figures are chosen to be relatively free of H_2O and H_2S lines. In the figures, H_2S lines are indicated by asterisks (*) and H_2O lines by circles (○).

VI. SUMMARY AND DISCUSSION

We report here an *ab initio* MRD-CI calculation of the dipole moment surfaces for the electronic ground state of the H_2Te molecule. Using the *ab initio* results, we calculate the vibrational transition moments (Tables 2–4), and we simulate the far infrared spectrum of H_2Te (Table 5, Figs. 3 and 4) by means of the MORBID program system (*19–23*).

The vibrational transition moments for H_2Te in Table 2 can be compared with the corresponding *ab initio* values for H_2S and H_2Se given in Refs. (*35*) and (*36*), respectively. It is found that for all vibrational transitions considered, the transition moment either increases monotonically or decreases monotonically for the sequence $H_2S \rightarrow H_2Se \rightarrow H_2Te$.

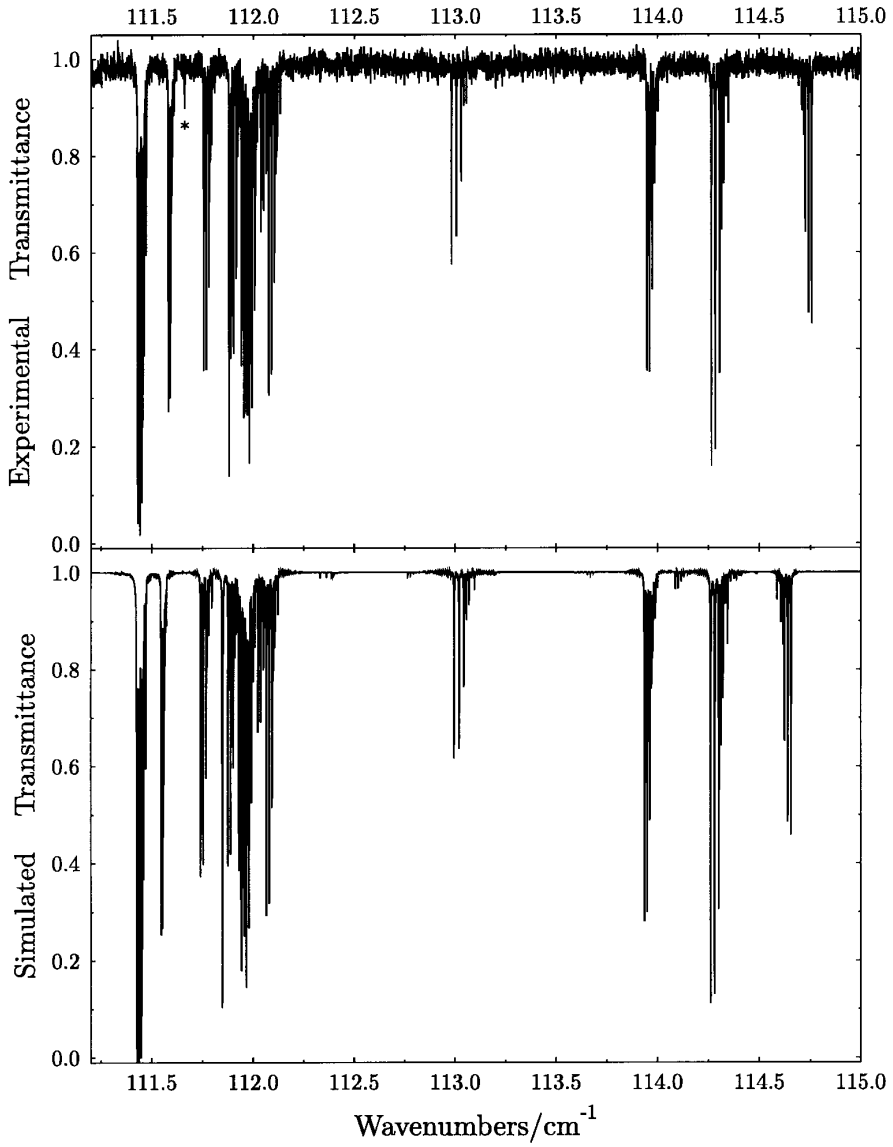

FIG. 3. A part of the experimental far-infrared transmittance spectrum of H_2Te (*5*) and the corresponding simulated spectrum. The asterisk (*) indicates an H_2S line.

For example, the transition moment for the ν_2 fundamental band is 0.015 Debye for H_2S, 0.051 Debye for H_2Se, and 0.111 Debye for H_2Te. Hence, the dipole moment surfaces calculated in the present work appear to fit well into the series of surfaces already determined for the related molecules H_2S and H_2Se. From the parameters of Ref. (*37*), the experimental value for the transition moment of the ν_2 fundamental band of H_2Se is obtained as (0.02947 $\pm$ 0.00070) Debye.

Table 5 showed that the absorbances calculated from the dipole moment surfaces of the present work are larger than the experimental absorbances by a factor of approximately 4. There are three possible reasons for this:

1. The equilibrium dipole moment value, obtained as 0.377 Debye from the parameters of Table 1 and the value $\rho_e = 89.58°$ (*1*) for the equilibrium $\bar{\rho}$ value, is too large. The intensities of the rotational transitions considered here are, to a good approximation, proportional to the square of the equilibrium dipole moment value. Hence, if the entire discrepancy between theory and experiment is attributed to inaccuracy of the dipole moment, we would obtain agreement with experiment by reducing the equilibrium dipole moment by a factor of $\sqrt{4.07} \approx 2.0$ resulting in a value of 0.19 Debye.

2. In our determination of the H_2Te concentration, we assume that at the beginning of the experiment, the cell contains pure H_2Te so that the initial pressure of 5.01 mbar is entirely due to this molecule. There are impurities in the

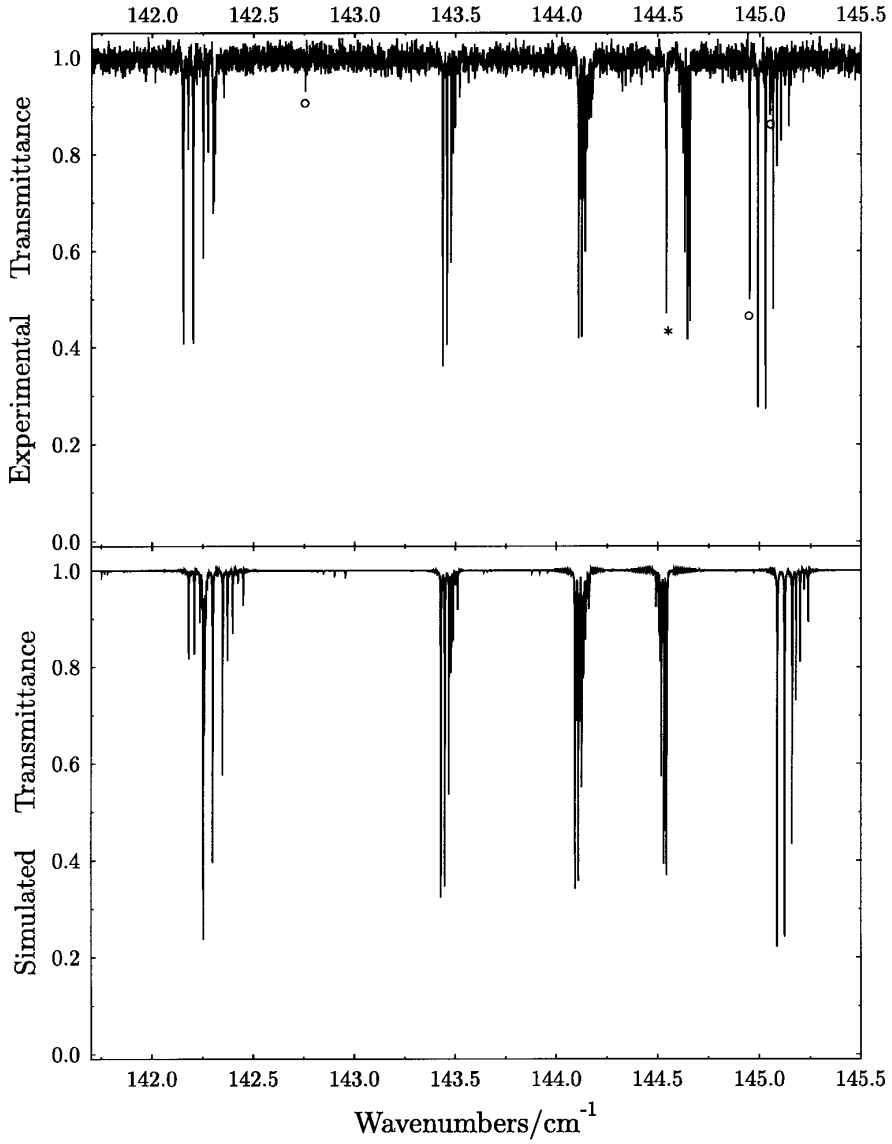

FIG. 4. A part of the experimental far-infrared transmittance spectrum of H_2Te (5) and the corresponding simulated spectrum. The asterisk (*) indicates an H_2S line and the circles (○) indicate H_2O lines.

sample (for example the H_2S and H_2O whose absorption lines we observe) which cause the initial partial pressure of H_2Te to be smaller than 5.01 mbar. Consequently, the H_2Te concentration c^* (Eq. [11]) used for the simulation is too high. If we assume the *ab initio* equilibrium dipole moment value to be correct, we must reduce c^* by a factor of 4.07 to obtain agreement with experiment.

3. In the simulation, we use a partition function value Q (Eq. [6]) obtained by summation over all energies, converged or not converged, generated in the MORBID calculation with the given basis set and J_{max} value. This Q value could be smaller than the true value obtained by summation over all energy levels, leading to integrated absorption coefficients (Eq. [5]) that are too large.

With the basis set and J_{max} value chosen for the MORBID calculation, the energy level spectrum is reasonably calculated up to approximately 8000 cm^{-1} above the vibrational ground state. Energies above this threshold contribute less than 10^{-21} to the partition function at the absolute temperature $T = 233$ K. Hence the Q value used in the simulation is believed to be quite accurate. The reason for the discrepancy between the observed and calculated absorbance values is presumably a combination of large values for both the equilibrium dipole moment and the H_2Te pressure. As mentioned above, we obtain a value of 0.19 Debye for the equilibrium dipole moment if we consider the H_2Te concentration used in the simulation to be correct. We can consider this value as a lower limit for the equilibrium dipole moment. Previous

experience (*38*) with the FTIR spectra of H_2Te from Refs. (*6, 7*) suggests that the actual partial pressure of H_2Te pressure may be as low as 50% of the initial pressure measured at the beginning of the experiment. This means that we should reduce the H_2Te concentration c^* (Eq. [11]) by a factor of 2. In this situation, we must still reduce the equilibrium value of the dipole moment by a factor of $\sqrt{4.07/2} \approx 1.43$ to obtain agreement with experiment. This produces a value of 0.26 Debye, which we can consider as a probable upper limit. Hence we conclude that the equilibrium dipole moment for H_2Te is certainly larger than 0.19 Debye and very probably smaller than 0.26 Debye. A more definitive assessment of the dipole moment for H_2Te awaits precise measurements by means of Laser Stark spectroscopy.

In considering the magnitude of the correction of the *ab initio* dipole moment necessary to obtain agreement with experiment, it should be noted that in *ab initio* dipole moment computations the absolute magnitude of the deviation from a given observed value tends to be constant from one molecule to another. This means that the percentage error can be quite high for a weakly polar molecule such as H_2Te, while for a strongly polar molecule it might be quite small and still represent the same level of accuracy. This fact must be kept in mind in judging the quality of the present results. Further, it should be noted that the deviation of the calculated dipole moment components from the ''true'' values are probably only weakly dependent on the molecular geometry. Hence the vibrational transition moments given in Tables 2–4, which are largely independent of the absolute value of the dipole moment, are expected to be better determined from the *ab initio* calculation than the equilibrium dipole moment.

There has been one previous *ab initio* calculation of the equilibrium dipole moment of H_2Te (*39*) producing the value of 0.27 Debye, which falls at the upper end of the interval given above. In this calculation, the variation of the dipole moment with molecular geometry was not investigated. We have attempted, by use of the same *ab initio* basis set (two additional Te *d* AO's) at the equilibrium geometry of H_2Te, to reproduce the value of Ref. (*39*). With this basis set, we do indeed obtain a lowering of the equilibrium dipole moment value to 0.309 Debye employing a selection threshold similar to that in the calculations first discussed ($T = 0.2\ \mu E_h$). Use of the larger AO basis with a ten times smaller configuration threshold ($T = 0.02\ \mu E_h$) produced a slightly smaller value of 0.298 Debye, only 0.030 Debye larger than that obtained in Ref. (*39*) and slightly above the upper limit of 0.26 Debye indicated by the experimental considerations.

When we empirically reduce our calculated absorbance values by a factor of 4.07, we obtain rather satisfactory agreement between calculated and observed transmittances (Figs. 3 and 4). Some residual deviations may be due to the fact that we use the same pressure broadening line profile (Eq. [8]) for all transitions. In reality, this profile presumably depends on J and K_a since this has been found to be the case for the water molecule (*40*), where the HWHM of the pressure broadening line profile, $\Delta\tilde{\nu}_P$ (Eq. [8]), depends strongly on the J and K_a values of the states involved in the transition. The transitions shown in Figs. 3 and 4 typically involve values of $J > 10$. The calculated transition wavenumbers result from a potential energy function obtained in a fitting to term values with $J \leqslant 5$ (*1*) derived from the older, medium-resolution spectra reported in Refs. (*24–30*). Consequently, the peak wavenumbers calculated for the lines in the figures will deviate up to 0.2 cm^{-1} from the experimental values. These discrepancies are significant on the wavenumber scale of Figs. 3 and 4 and cause some details of the calculated and observed spectra to be visibly different. We hope that by fitting the improved experimental data from Refs. (*5–7, 9*) we shall be able to obtain a more accurate potential energy function which will remove some of these discrepancies.

ACKNOWLEDGMENTS

We are very grateful to H. Bürger and B. P. Winnewisser for helpful discussions and advice. Further, we thank H. Bürger and O. Polanz for permitting us to reproduce the experimental far infrared spectrum of H_2Te with which we have compared our theoretical calculations in Section V, J. Vander Auwera and M. Carleer for making the program SPECTRA available to us, and P. R. Bunker, H. Bürger, W. P. Kraemer, V. Špirko, and B. P. Winnewisser for critically reading the manuscript and suggesting improvements. This work was supported in part by the Deutsche Forschungsgemeinschaft (through Forschergruppe Grants Bu 152/12-4 and Bu 152/12-5), by the European Commission through Contract CHRX-CT94-0665 ''Highly Excited Rovibrational States,'' and by the Fonds der Chemischen Industrie. I.N.K. is grateful to the Deutscher Akademischer Austauschdienst for a fellowship.

REFERENCES

1. P. Jensen, G. Osmann, and I. N. Kozin, *in* ''Advanced Series in Physical Chemistry: Vibration-Rotational Spectroscopy and Molecular Dynamics'' (D. Papoušek, Ed.). World Scientific, Singapore, in press.
2. I. N. Kozin, S. P. Belov, O. L. Polyansky, and M. Yu. Tretyakov, *J. Mol. Spectrosc.* **152,** 13–28 (1992).
3. I. N. Kozin, S. Klee, P. Jensen, O. L. Polyansky and I. M. Pavlichenkov, *J. Mol. Spectrosc.* **158,** 409–422 (1993).
4. J.-M. Flaud, C. Camy-Peyret, H. Bürger, P. Jensen, and I. N. Kozin, *J. Mol. Spectrosc.* **172,** 194–204 (1995).
5. I. N. Kozin, P. Jensen, O. Polanz, S. Klee, L. Poteau, and J. Demaison, *J. Mol. Spectrosc.*, in press.
6. H. Bürger, J.-M. Flaud, L. Halonen, and O. Polanz, in preparation.
7. J.-M. Flaud, H. Bürger, and O. Polanz, in preparation.
8. P. Jensen, Y. Li, G. Hirsch, R. J. Buenker, T. J. Lee, and I. N. Kozin, *Chem. Phys.* **190,** 179–189 (1995).
9. J. Demaison, H. Bürger, M. Paplewski, and O. Polanz, unpublished results.
10. K. Raghavachari, G. W. Trucks, J. A. Pople, and M. Head-Gordon, *Chem. Phys. Lett.* **157,** 479–483 (1989).
11. R. J. Buenker and S. D. Peyerimhoff, *Theo. Chim. Acta* **35,** 33–58 (1974).

12. R. J. Buenker and S. D. Peyerimhoff, *Theo. Chim. Acta* **39,** 217–228 (1975).
13. R. J. Buenker, S. D. Peyerimhoff, and W. Butscher, *Mol. Phys.* **35,** 771–791 (1978).
14. R. J. Buenker, *in* ''Proceedings of the Workshop on Quantum Chemistry and Molecular Physics, Wollongong, Australia'' (P. Burton, Ed.). University Press, Wollongong, 1980.
15. R. J. Buenker, *in* ''Studies in Physical and Theoretical Chemistry, Vol. 21, Current Aspects of Quantum Chemistry'' (R. Carbo, Ed.). Elsevier, Amsterdam, 1981.
16. R. J. Buenker and R. A. Phillips, *J. Mol. Struct. THEOCHEM* **123,** 291–300 (1985).
17. M. M. Hurley, L. F. Pacios, and P. A. Christiansen, *J. Chem. Phys.* **84,** 6840–6853 (1986).
18. T. H. Dunning, Jr., *J. Chem. Phys.* **90,** 1007–1023 (1989).
19. P. Jensen, *J. Mol. Spectrosc.* **132,** 429–457 (1988).
20. P. Jensen, *J. Mol. Spectrosc.* **128,** 478–501 (1988).
21. P. Jensen, *J. Chem. Soc. Faraday Trans. 2* **84,** 1315–1340 (1988).
22. P. Jensen, *in* ''Methods in Computational Molecular Physics'' (S. Wilson and G. H. F. Diercksen, Eds.). Plenum, New York, 1992.
23. P. Jensen, *in* ''Molecules in the Stellar Environment'' (U. G. Jørgensen, Ed.), Lecture Notes in Physics 428. Springer-Verlag, Berlin, 1994.
24. K. Rossmann and J. W. Straley, *J. Chem. Phys.* **24,** 1276–1277 (1956).
25. R. A. Hill, T. H. Edwards, K. Rossmann, K. Narahari Rao, and H. H. Nielsen, *J. Mol. Spectrosc.* **14,** 221–243 (1964).
26. N. K. Moncur and T. H. Edwards, *J. Chem. Phys.* **51,** 2638–2640 (1969).
27. N. K. Moncur, P. D. Willson, and T. H. Edwards, *J. Mol. Spectrosc.* **52,** 181–195 (1974).
28. P. D. Willson, N. K. Moncur, and T. H. Edwards, *J. Mol. Spectrosc.* **52,** 196–208 (1974).
29. N. K. Moncur, P. D. Willson, and T. H. Edwards, *J. Mol. Spectrosc.* **52,** 380–391 (1974).
30. A. V. Burenin, A. F. Krupnov, S. V. Mart'yanov, A. A. Mel'nikov, and L. I. Nikolayev, *J. Mol. Spectrosc.* **75,** 333–337 (1979).
31. J. W. C. Johns, *Mikrochim. Acta (Wien)* **111,** 171–188 (1987).
32. B. Jancovici, ''Statistical Physics and Thermodynamics.'' McGraw-Hill, London, 1973.
33. L. Faires, *Anal. Chem. A* **58,** 1023–1034 (1986).
34. I. M. Mills, T. Cvitaš, K. Homann, N. Kallay, and K. Kuchitsu, ''Quantities, Units and Symbols in Physical Chemistry.'' Blackwell Scientific, London, 1993.
35. J. Senekowitsch, S. Carter, A. Zilch, H.-J. Werner, N. C. Handy, and P. Rosmus, *J. Chem. Phys.* **90,** 783–794 (1989).
36. J. Senekowitsch, A. Zilch, S. Carter, H.-J. Werner, P. Rosmus, and P. Botschwina, *Chem. Phys.* **122,** 375–386 (1988).
37. J.-M. Flaud, P. Arcas, C. Camy-Peyret, H. Bürger, and H. Willner, *J. Mol. Spectrosc.* **166,** 204–209 (1994).
38. H. Bürger, private communication.
39. K. Sumathi and K. Balasubramanian, *J. Chem. Phys.* **92,** 6604–6619 (1990).
40. T. Giesen, R. Schieder, G. Winnewisser, and K. M. T. Yamada, *J. Mol. Spectrosc.* **153,** 406–418 (1992).